ACS APPLIED MATERIALS & INTERFACES

Research Article

www.acsami.org

Silica Cross-linked Micelles Loading with Silicon Nanoparticles: Preparation and Characterization

Guo-Hui Pan,*[,†] Alexandre Barras,[†] Luc Boussekey,[‡] and Rabah Boukherroub*[,†]

[†]Institut de Recherche Interdisciplinaire, CNRS USR 3078, Université Lille 1, Parc de la Haute Borne, 50 avenue de Halley, 59658 Villeneuve d'Ascq, France

[‡]Laboratoire de Spectrochimie Infrarouge et Raman, CNRS UMR 8516, Université Lille 1, 59655 Villeneuve d'Ascq, France

Supporting Information

ABSTRACT: A new family of luminescent and stable silicon-based nanoparticles (NPs), silica cross-linked pluronic F127 (PF127) micelles loaded with decyl capped silicon nanoparticles (decyl-SiNPs), were synthesized in aqueous media. The decyl-SiNPs were prepared by first liberating hydride terminated SiNPs (H-SiNPs) from a porous silicon matrix followed by their functionalization via hydrosilylation with 1-decene under photochemical activation. The silicon-based NPs exhibit bright photoluminescence (PL) with a quantum yield of ~3.8% and peaking at ~2.0 eV, which lies within the transmission window that is useful for biological imaging. They display a hydrodynamic size of ~25 nm with exterior polyethylene oxide (PEO) blocks stretching out in aqueous media. Chloroform was found to quench the excitation at energy above 4.9 eV by shielding the incident light or relaxing the charge carriers, which highlights that caution against solvent interference should be taken when performing the studies on PL origin and luminescence efficiency of SiNPs. For PF127, the blocks of hydrophilic PEO participate in the PL quenching, while poly(propylene oxide) (PPO) does not. The colloidal solution displays excellent PL stability against salt (NaCl) and temperature but is susceptible to basic solution at pH above 9.

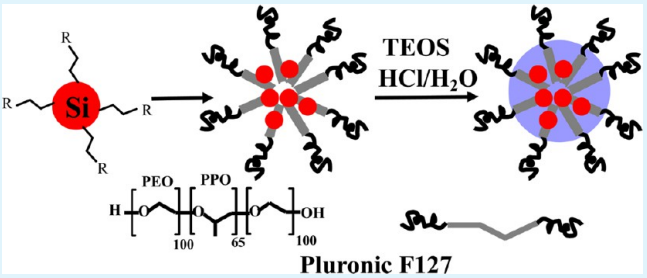

KEYWORDS: *silicon nanoparticles, photoinitiated hydrosilylation, micelles loading, water solubility, photoluminescence, solvent quenching*

1. INTRODUCTION

The pioneering discovery by Canham[1] of the visible luminescence in porous silicon at room temperature and subsequent demonstrations[2,3] on its inherent complex nanoscale architecture correlated with the bright emission greatly changed the conventional idea that silicon is only of particular importance in electronics but not of potential in optoelectronics. This finding also stimulated significant research effort in nanoscale silicon, including synthesis, surface modification, origin of luminescence, and applications (e.g., chemical sensors, optoelectronic devices, electroluminescent displays, photodetectors, lasing material for photo pumped tunable lasers, fluorescence labeling and biological imaging, cancer therapy, etc).[4−8] Nanoscale silicon features benignity, abundance, bright photoluminescence, biocompatibility, and biodegradability in nature. These properties made silicon nano-objects potential candidates for bioimaging by comparison with other alternative quantum dots such as, Cd and Pb containing compounds that are potentially toxic due to Cd^{2+} and Pb^{2+} leaching. In contrast, silicon is of intrinsic nontoxicity given the fact that it is a common trace element in humans and could be naturally absorbed and extracted by some different tissues.[9−11]

Water dispersibility is one necessary characteristic of nanoparticles (NPs) for any sought after utilization in biomedicine. The same is true for silicon nanoparticles (SiNPs). In principle, water-dispersible SiNPs can be prepared via hydrosilylation reaction of hydrogenated SiNPs with ω-functionalized 1-alkene (i.e., one end with carbon−carbon double bond, the other distal end with hydrophilic polar groups, for instance, acid, hydroxyl, amine groups). However, to date, due to the low quality of surface monolayers and low surface coverage, there are only a few reports on this kind of surface modification that successfully suppressed the quick luminescence degradation and flocculation in aqueous solution.[12−16] In contrast, alkyl passivation yields high quality of surface capping and, thus, prevents the silicon core from oxidation by oxygen and moisture.[17−19] This alkyl grafting imparts hydrophobicity to the SiNPs and allows high dispersion in some nonpolar solvents. A second chemical treatment is, however, essential to facilitate their dispersion in aqueous solution. Up to now, this two-step strategy has received substantial consideration to produce aqueous dispersions of luminescent SiNPs. A dispersing agent such as phospholipid micelle,[20,21] solid lipid nanoparticles,[22] amphiphilic polymer,[23,24] or polymer nanoparticles,[25] has been employed to coat the hydrophobic alkylated surface.

Received: April 11, 2013
Accepted: July 11, 2013
Published: July 11, 2013

   dx.doi.org/10.1021/am401313x | ACS Appl. Mater. Interfaces 2013, 5, 7042−7049

For successful in vivo studies, such as cancer imaging or therapy involving quantitative real-time study of transport parameters of NPs-based drugs, the development of in situ tissue microenvironment probes, the measurement of living tissue microrheology,[26] etc., design of nanoparticle vectors should also take into account the following minimum criteria: colloidal stability, low protein adsorption, high signal-to-background levels, and small enough size to circulate the bloodstream for extended time. NPs were generally encapsulated in molecular layers such as lipids, polyethylene glycol (PEG), or amphiphilic polymers that "disguise" them from being recognized as foreign bodies (nonimmunogenic and/or nonantigenic) and thereby prolong their half-life in the bloodstream.[24] Previous studies also indicated that particles larger than 100 nm would be quickly removed from the blood by cells of the reticuloendothelial system (RES), while NPs smaller than 5.5 nm in diameter would be rapidly filtered by the kidney; the optimal size for crossing cell membranes via receptor-mediated endocytosis is between 25 and 50 nm.[24]

The work presented herein aims to develop a simple two-step method for producing stable silicon-based NPs in aqueous medium and to study the influence of the coating on their photoluminescence (PL) properties. The technique relies on the encapsulation of red-emitting SiNPs, chemically modified with decyl groups, into silica cross-linked pluronic F127 (PF127) micelles. PF127 is an ABA-type triblock copolymer consisting of hydrophobic poly(propylene oxide) (PPO) and hydrophilic polyethylene oxide (PEO) segments. In an aqueous environment, it has been demonstrated that these molecules can self-assemble into spherical, hydrophobic PPO core/hydrophilic PEO shell-like particles above the critical micelle concentration (CMC).[27] Small-sized and hydrophobic silicon NPs could thus be entrapped into the core of the micelles through hydrophobic van der Waals interactions between the decyl groups and PPO blocks. Subsequent silica cross-linking in the interior PEO blocks region of the PF127 micelle can strengthen the micellar structure for a long-term stability against dissociation readily upon dilution in body fluids, interaction with polar biomolecules encountered in in vivo studies, and elevated temperature, leaving the exterior PEO blocks stretched out in aqueous media.[27] The PEO blocks could present a high biocompatibility by effectively preventing aggregation, adsorption of proteins, adhesion to tissues, and recognition by the RES primarily in the liver and spleen.[27−32] Likewise, the selected hybrid coating materials of PF127 copolymer and silica are both highly safe in vivo and have been approved by the Food and Drug Administration.[32,33] After encapsulation, the resulting silicon-based NPs bear bright red emission located in the transparent window of biological tissue (650−900 nm) useful for in vivo imaging,[24] and a hydrodynamic size of ∼25 nm falling into the superior hydrodynamic size range for prolonging half-life in the bloodstream.

Additionally, PL studies on silicon nanocrystallites are still an active subject for research. Although quantum confinement effects are generally accepted to be responsible of the PL, physical origin of light emission is still an ongoing issue of debate.[5,8,14,34−42] Up to now, there is no conclusive and definitive classification on various PL behaviors, including broad emission bands spanning from the UV to infrared spectral region and fluorescence dynamics greatly varying from microseconds to nanoseconds, observed on the basis of different sizes, surface chemistry, and methods of synthesis.[34−42] Discussions are mainly focused on whether decreasing the size changes the indirect band gap character, and thereby, the light emission in ultrasmall sized Si is generated by recombination via direct band gap or whether the PL is produced by excitonic transitions inside nanoscale silicon or by other surface-related centers.[34−42] In contrast to the silicon indirect band gap, more extensive and further-reaching research has yielded a detailed fundamental understanding of PL properties of direct band gap II−VI (e.g., CdSe, CdTe, CdS, etc.) and III−V (e.g., InP, InAs, etc.) quantum dots (QDs).[43] A consensus has been achieved on the basis of quantum confinement effects for their PL characteristics and the steepness of the absorption onset, size-dependent narrow absorption and emission bands, and nanosecond magnitude of fluorescence lifetime, which were generally observed in high quality QDs.[43]

In this paper, we found that chloroform quenched the excitation at energy above 4.9 eV by shielding the incident light or relaxing the charge carriers. This highlights that caution against solvent interference should be taken when performing studies on PL origin and luminescence efficiency of SiNPs. Moreover, the PL properties dependence on salt concentration (NaCl), temperature, and pH were also investigated on a colloidal solution of decyl-SiNP loaded silica cross-linked PF127 micelles. The colloidal solution displays excellent PL stability against salt (NaCl) and temperature but is susceptible to basic solution at pH above 9.

2. EXPERIMENTAL SECTION

2.1. Materials and Reagents. P-type (100) crystalline silicon wafers (Siltronix, B-doped, 0.009−0.01 Ω cm resistivity and 355−405 μm in thickness) were used as substrates for the preparation of porous silicon. Sulfuric acid (96%, H_2SO_4), hydrofluoric acid (48%, HF), and hydrogen peroxide (30%, H_2O_2), 1-decene (≥97%), tetraethyl orthosilicate (TEOS), vanadium oxide (V_2O_5), pluronic F127 (PF127), diethoxydimethylsilane (DEDMS, 97%), hydrochloric acid (HCl), absolute ethanol, methanol, anhydrous toluene, anhydrous chloroform and Celite®560 coarse were all purchased from Sigma-Aldrich. Deionized water was obtained from a Milli-Q plus system (Millipore, Paris, France). Toluene was dried over Na overnight prior to use. 1-Decene was purified immediately before use by passing over dried Celite column to remove inhibitor and/or peroxide impurities.

2.2. Synthesis of Decyl-Terminated Si Nanoparticles (Decyl-SiNPs). Briefly, p-type prime grade Si (100) wafers were first cleaned ultrasonically in ethanol and acetone, rinsed with Milli-Q water, and then cleaned in a piranha solution (3:1 concentrated H_2SO_4/30% H_2O_2) for 30 min followed by copious rinsing with Milli-Q water. Then, the clean wafer was dipped into a solution containing HF (48%, 5 mL) and V_2O_5 (0.22 g) for 12 h chemical etching at room temperature.[44] Etching was performed under N_2 and the dead volume in the containers was always filled with N_2 to reduce the effects of dissolved O_2 and CO_2. The resulting porous silicon was in turn washed with 5% HF, a large amount of 1:3 methanol/water mixture and pure methanol to remove any adsorbed acid and other impurities, and finally dried with N_2. After cleaning, the porous silicon was immediately placed into previously deoxygenated (by bubbling with N_2) solution of 1-decene and toluene followed by ultrasonication (Branson 2510) for 3 h and photoinitiated hydrosilylation for 2 h under 254 nm irradiation. After reaction, the small-sized decyl-SiNPs were collected in the supernatant by centrifugation (4000 rpm, Eppendorf 5810 R) for 40 min. Decyl-SiNPs were purified by several cycles of precipitation/resuspension with ethanol and, then, were dispersed in pure chloroform and passed through 0.22 μm syringe filter (PTFE).

Safety Considerations. The mixture H_2SO_4/H_2O_2 (piranha) solution is a strong oxidant. It reacts violently with organic materials. It can cause severe skin burns. It must be handled with extreme care in

a well-ventilated fume hood while wearing appropriate chemical safety protection.

Caution! HF is a hazardous acid which can result in serious tissue damage if burns are not appropriately treated. Etching of silicon should be performed in a well-ventilated fume hood with appropriate safety considerations: face shield and double layered nitrile gloves.

2.3. Loading of Decyl-SiNPs into Silica Cross-linked PF127 Micelles. Following a slightly modified procedure developed previously,[27−31] decyl capped SiNPs were loaded into silica cross-linked PF127 micelles. In a typical preparation, 0.2 g of PF127 was carefully solubilized in 1−2 mL of chloroform with 1.0 mg decyl-SiNPs in a 20 mL glass tube. The solvent was evaporated from the homogeneous solution by means of a gentle nitrogen flow and subsequently under vacuum at room temperature. NaCl (137 mg) was added to the solid residue, and the mixture was solubilized at 25 °C under magnetic stirring with 3.2 mL of 0.85 M aqueous hydrochloric acid solution. TEOS (0.36 mL, 1.61 mmol) was then added to the resulting aqueous homogeneous solution under stirring, followed by diethoxydimethylsilane (DEDMS, 97%, 30 μL) after 3 h. The mixture was kept under stirring for 20 h at 25 °C before dialysis treatment. The dialysis purification step was carried out against water. The NP solution was filtered through a Teflon filter (0.22 μm) to remove the possible large particles. The loading rate of decyl-SiNPs is roughly estimated to be ∼0.34 wt % by assuming the complete loading of decyl-SiNPs and full hydrolysis of TEOS to silica.

2.4. Characterization. *2.4.1. Fourier Transform Infrared Spectroscopy (FTIR).* FTIR spectra were recorded using a ThermoScientific FTIR instrument (Nicolet 8700) with a resolution of 4 cm^{-1} using KBr pellet techniques. Sixteen accumulative scans were collected.

2.4.2. Transmission Electron Microscopy (TEM). TEM images were obtained on a JEM- 2100F microscope operating at 200 kV. Samples were drop-cast from chloroform or aqueous dispersions onto a carbon-coated TEM grids, and the solvent was evaporated under gentle heating by a lamp.

2.4.3. UV−vis Absorption Spectrometry. UV−vis absorption spectra were conducted on a Perkin-Elmer Lambda 950 dual beam spectrophotometer operating at a resolution of 1 nm in the region 200−800 nm.

2.4.4. Size and Zeta Potential. The average diameter and polydispersity index (PdI) were determined by dynamic light scattering using a Zetasizer Nano ZS (Malvern Instruments S.A., Worcestershire, UK) instrument in 173 °C scattering geometry. Zeta potential of the particles was measured using the electrophoretic mode of Zetasizer Nano ZS.

2.4.5. PL Spectroscopy. Fluorescence and excitation spectra were recorded on a Hitachi F-4600 spectrophotometer equipped with a 150 W Xe-arc lamp and a 450 nm emission cutoff filter at room temperature. For comparison, the spectra were measured at a fixed bandpass of 0.2 nm with the same instrument parameters (2.5 nm for excitation split, 2.5 nm for emission split, and 700 V for PMT voltage). The PL spectra of decyl-SiNPs chloroform dispersion and decyl-SiNPs@PF127@SiO_2 NPs aqueous solution were recorded after 6 months of storage in the dark. The PL dependence studies on pH, temperature, and salt concentration were performed after storage for 5 more months. Different concentrations of colloidal solution were used during the measurements.

To investigate the temperature dependence of the decyl-SiNPs@PF127@SiO_2 NPs' PL, the colloidal aqueous solution was heated in an oven ranging from ambient temperature (25 °C) to 100 °C. At a given temperature, the NP solution was maintained for 4 min, and then, the fluorescence spectrum was recorded immediately upon excitation at 270 nm.

To investigate the pH dependence of the decyl-SiNPs@PF127@SiO_2 NPs' PL, the pH of the NP aqueous dispersion was tuned from 2 to 12 by dropwise addition of an appropriate amount of HCl (0.01, 0.1, and 1.0 M) or NaOH (0.01, 0.1, and 1.0 M), then the fluorescence emission spectra were recorded immediately upon excitation at 270 nm. The pH was monitored with a Pengshun PHS-3C multi-pH meter.

To investigate the influence of the salt concentration on the decyl-SiNPs@PF127@SiO_2 NPs' PL properties, an appropriate amount of NaCl was added into the NP aqueous dispersion with the salt concentration varying from 0 to 1.0 mol/L, and then, the fluorescence emission spectra were recorded immediately upon excitation at 270 nm.

2.4.6. Fluorescence Quantum Yield (QY). Before storage, photoluminescence quantum yield (PL-QY) measurements were performed at room temperature using a Hamamatsu Photonics C11347-11 absolute PL-QY system equipped with integrating sphere, photonic multichannel analyzer, and 350-nm line of the xenon lamp.

3. RESULTS AND DISCUSSION

Porous silicon has been demonstrated to be a complex network of nanocrystallites, and the origin of its PL arises from the quantum confinement within the nanostructures comprising this material. The porous matrix can be easily prepared by chemical or electrochemical dissolution of silicon in HF-based solutions with controlled pore size, thickness, and porosity over a wide range.[45] A variety of methods have been developed for the synthesis of silicon NPs.[5,6] Perhaps liberating from porous silicon via physical fracture is the most widely adopted technique for generating H-passivated silicon NPs. Porous silicon can be produced by stain etching by exposure of a crystalline silicon wafer to an aqueous mixture of hydrofluoric acid and an oxidant, in which the reactions are driven by the difference in the electrochemical potential between the Si and the electrolyte. Nitric acid (nitrate or nitrite) is almost exclusively used as the oxidant.[44] Recent studies have shown that an oxidant that involves a transition metal ion, e.g. Fe(III), Ce(IV), V(V), and Mn(VII) could be used instead.[44,46−48] In the present study, an aqueous solution of V_2O_5 and HF was employed to prepare porous silicon. In this process, it was suggested that VO_2^+ ions collide with the surface of the wafer, then inject holes into the silicon valence band, and thereby initiate the etching reaction as well as pore formation through random nucleation then lengthening linearly in time.[44]

The obtained porous silicon was broken up into individual hydride-terminated NPs by ultrasonication in a 1-decene containing toluene solution. Subsequent ultraviolet (UV) irradiation initiated the hydrosilylation reaction to give decyl passivated SiNPs via a robust Si—C covalent linkage. The FTIR spectrum of decyl-SiNPs is shown in Figure 1. It consists of characteristic vibrations of alkyl chains (symmetric bending modes of Si—CH_2 at ∼1261 cm^{-1}, CH_3 symmetric deformations at 1378 cm^{-1}, CH_3 asymmetric mode/CH_2 deformations at 1465 cm^{-1}, and strong C—H_x stretching

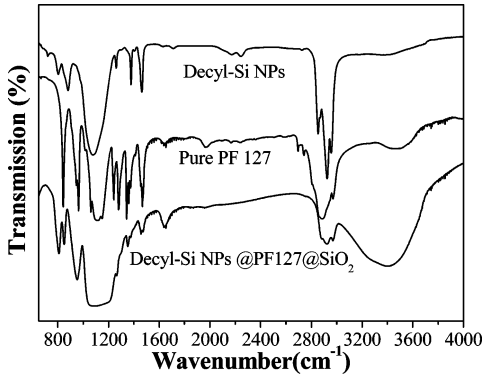

Figure 1. FTIR spectra of decyl-terminated SiNPs, pure PF127, and decyl-SiNPs@PF127@SiO_2 NPs.

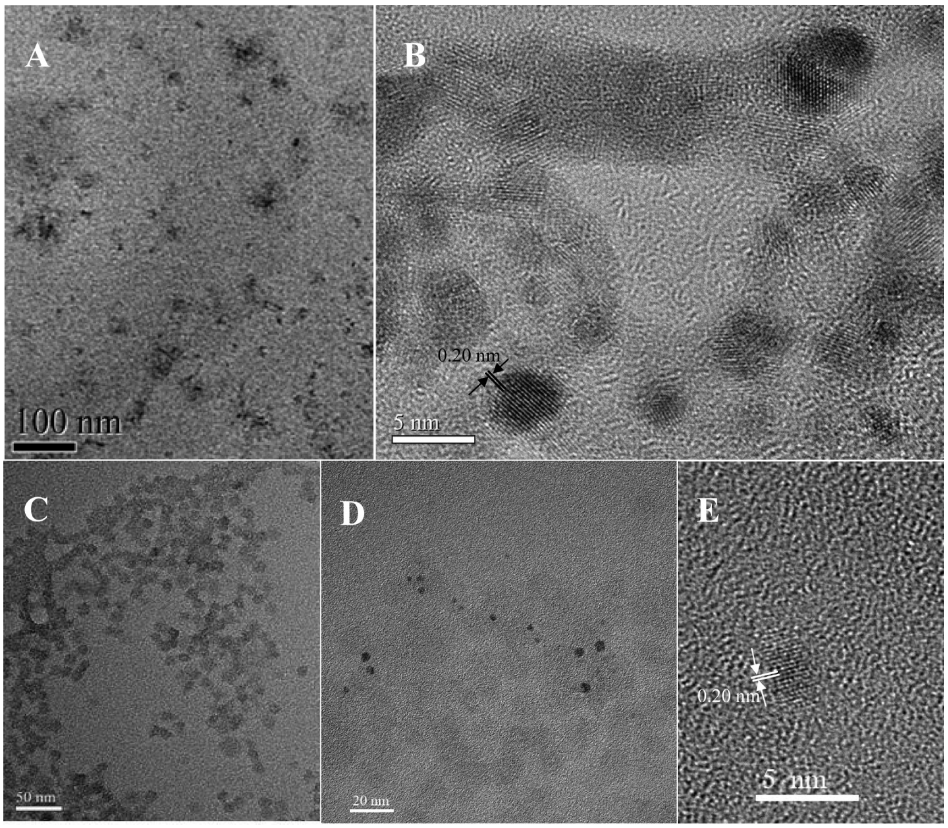

Figure 2. TEM images of decyl-terminated SiNPs (A, B) cast from a chloroform dispersion and decyl-SiNPs@PF127@SiO_2 NPs (C–E) cast from water. (D) High magnification TEM image, where some SiNPs in the form of darker spots were visualized inside the micelles. (E) One crystalline SiNP.

modes in the range 2800–3000 cm^{-1}). The absence of bands related to C═C double bond stretching, generally located at ~1641 cm^{-1}, and Si—H stretching at around 2100 cm^{-1} is a good indication that the hydrosilylation reaction took place on the SiNPs surface.[18,49] The presence of a broad and weak absorption band centered at 1080 cm^{-1} assigned to Si—O—Si species (stretching mode) suggests that only a small fraction of the surface was oxidized, which most likely occurred during the ambient atmosphere clean up of porous silicon. The FTIR spectrum of pure PF127 was also exhibited in Figure 1. It is more complex with some specific bands at 842 and 1112 cm^{-1} assigned to the stretching vibration of C—O—C; the bands at 1289 and 1344 cm^{-1} due to the bending vibrations of C—H are associated with the PEO segments.[50,51] After encapsulating decyl-SiNPs into the silica cross-linked micelles (decyl-SiNPs@PF127@SiO_2), the FTIR spectrum is dominated by the characteristic peaks of both silica network (Si—O—Si stretch at 1080 cm^{-1}) and copolymer. The peaks from decyl-SiNPs overlap with that of the polymer.

Figure 2A shows a low magnification TEM image of decyl-SiNPs cast from a chloroform dispersion. It displays individual particles less than 10 nm in diameter without any much larger particles and significant aggregation. Due to the extremely small size and relatively low electron density contrast to carbon background, some decyl-SiNPs are nearly transparent to electron beam so that they cannot be imaged easily, which usually makes TEM observation experimentally challenging.[14,24] On the same sample, some clear lattice-fringes of highly crystalline decyl-SiNPs of 2–7 nm in size were successfully imaged (Figures 2B). The observed *d*-spacing of 0.20 nm is in good agreement with the lattice spacing of the (220) plane of cubic silicon nanocrystals. Since the NPs are released into solution from porous silicon, they are expected to be polydisperse in size. Following our procedure described in the Experimental Section, small sized objects can be selectively collected, which favors the facile loading into the core of copolymer micelles with a small spatial volume, and without restructuring the micellar domains (e.g., by modulating assembly formulation and size). After encapsulation, the decyl-SiNPs@PF127@SiO_2 NPs can be easily imaged with a size of ~10 nm and a high monodispersity (Figure 2C). The size is in good agreement with previous reports.[27−31] It implies that decyl-SiNPs guests were entrapped into the micelles without remarkably increasing the whole size of the host materials. It differs from the case of iron oxide NP loading reported previously,[32] where the size was increased greatly after loading due to the bigger size of encapsulated NPs. This further gives evidence that the as-prepared decyl-SiNPs are extremely small in size, even smaller than the core diameter of the micelles. Additionally, upon extensive examination under high resolution TEM (Figure 2D and E), some silica cross-linked micelles were observed to encapsulate some crystalline decyl-SiNPs in the form of darker spots. The decyl-SiNP particles are randomly distributed in the center or near the surface of the micelles. On the other hand, some micelles seem to be empty inside; perhaps they are embedded by low-contrast decyl-SiNPs or are decyl-SiNP-free due to the inhomogeneity of encapsulation. Figure 3A shows the size distribution of decyl-SiNPs by numbers before and after encapsulation measured by DLS in chloroform and water, respectively. The decyl-SiNPs

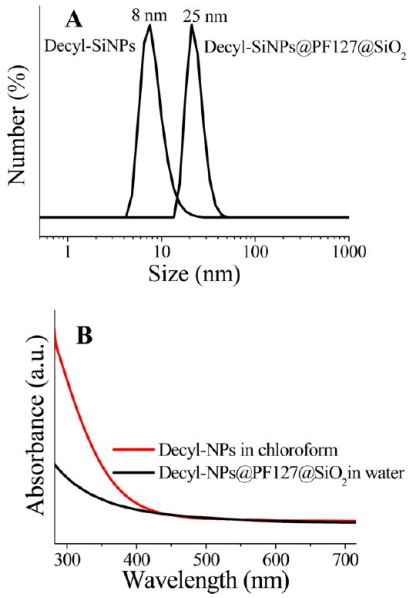

Figure 3. (A) Size distribution of decyl-SiNPs in chloroform and decyl-SiNPs@PF127@SiO_2 NPs in water. (B) Absorption spectra of decyl-SiNPs before and after encapsulation into silica cross-linked micelles.

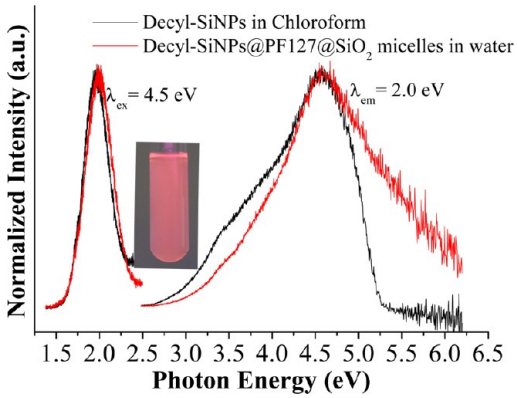

Figure 4. PL excitation and emission spectra of decyl-SiNPs before and after encapsulation into silica cross-linked micelles. All of the spectra were normalized to the maxima. Inset is a photograph of the decyl-SiNPs@PF127@SiO_2 NP aqueous dispersion under UV (365 nm) irradiation. The emission spectra were recorded with excitation energy of 4.5 eV; the excitation spectra were recorded at emission energy of 2.0 eV.

exhibit a good dispersion in chloroform with a particle size of ~8 nm (PdI: 0.246). After encapsulation, the particle size increased to ~25 nm (PdI: 0.325, zeta potential: −7.4 mV). The hydrodynamic diameter is larger than the diameter measured by TEM because the light scattering measurement includes the contribution of the decyl ligands and PEO chains both extended in the solution, which showed no contrast in the TEM study.[27,52] The TEM images of the NPs suggest that the silica cores present sufficient contrast to appear in the images.

Absorption spectra of decyl-SiNPs in chloroform and decyl-SiNPs@PF127@SiO_2 in water are displayed in Figure 3B. Both spectra have nearly the same onset at ~500 nm, which is significantly blue-shifted by comparison with bulk silicon due to the quantum confinement effects. The decyl-terminated SiNPs are highly hydrophobic and can be readily dispersed into chloroform via slight sonication and give rise to a clear yellowish solution. For NP dispersions, their absorption spectra generally represent the contribution of both absorption and scattering of dispersed NPs to the incident light. Herein, the same absorption onset observed for decyl-SiNPs@PF127@SiO_2 aqueous dispersion means that these NPs are still small enough and highly dispersible in water without severe aggregation or flocculation, which usually scatters the incident light significantly and yields the spectral intensity in the collected spectra. The high dispersion of decyl-SiNPs@PF127@SiO_2 is assigned to the exterior PEO blocks stretched out in aqueous media. This result is in accordance with previously reported data on silica cross-linked PF127 block copolymer micelles loaded with organic dyes and magnetic NPs.[27,32]

The SiNPs liberated from porous silicon exhibit bright red emission under UV excitation. The absolute PL quantum yield (PL-QY) was determined to be ~8.0% after surface passivation with decyl chains. Loading into the silica cross-linked micelles maintained the red emission (see photograph in Figure 4), but with a decrease in PL-QY to ~3.8%. The highest PL-QY of indirect band gap SiNPs has been reported to be 60%,[53] while the values are much higher for direct band gap quantum dots (QDs): up to 85% for orange-red-emitting CdSe[54] and even near 100% for green-emitting CdSe/CdS[55] at room temperature. The colloidal aqueous solution is stable for more than 11 months without obvious flocculation. The PL intensity shows no appreciable change after 5 months of storage in the dark at room temperature (Supporting Information Figure S1). The colloidal and PL stability gives another support for successful loading of decyl-SiNPs. Figure 4 shows the excitation and emission spectra of decyl-SiNPs chloroform dispersion and decyl-SiNPs@PF127@SiO_2 aqueous dispersion. The emission of decyl-SiNPs ranges from 1.5 to 2.5 eV with a peak shift at 1.95 and 2.0 eV for decyl-SiNPs in chloroform and decyl-SiNPs@PF127@SiO_2 in water, respectively. According to the quantum confinement model,[56−59] the PL peak energy at 2.0 eV corresponds to ~2.9 nm NP diameter. In contrast, the efficient excitations are located at a much higher energy region extending from 2.45 to 6.0 eV and peaking at the same photon energy of 4.56 eV, which is fairly similar to a previous study.[60] By turning the attention back to the UV−vis absorption spectra, the weak absorption that monotonically increases with increasing energy from the onset at ~2.5 eV is the characteristic of absorption across the indirect band gap of silicon,[14] that is, in spite of smaller size these SiNPs still maintain the intrinsic nature of indirect band gap like bulk silicon. In addition, the PL excitation spectra compare very well with the absorption spectra of SiNPs, which means that the PL is well-correlated with the absorption of light by the core of the NPs rather than other impurities.[59,60] In terms of the big stokes shift occurring in SiNPs, i.e., much higher excitation energy than that of emission, the direct interband high-energy transition at Γ (Γ → Γ, 3.4 eV for bulk silicon) or L (L → L, 4.4 eV for bulk silicon) in the deep UV and vacuum ultraviolet (VUV) spectral regions in SiNPs should be responsible for the observed excitation spectra.[61] Therefore, it was suggested that the intense PL results from efficient generation of electron−hole pairs in the SiNPs via direct transition, followed by recombination within the NP core via an indirect transition or through surface states whose energies are coupled to the indirect band gap energy.[59]

Moreover, in stark contrast to the aqueous dispersion, the chloroform dispersion of decyl-SiNPs shows a dramatic

quenching at higher energy above 5.0 eV in the PL excitation spectrum. One can easily conclude that the variation of local environment surrounding decyl-SiNPs induced the PL quenching in the region of high energy. Over the two systems, the surrounding medium of decyl-SiNPs changes from chloroform to micelles where PF127 copolymer is the closest species to interact with SiNPs and silica is the second-closest one. Silica is not usually considered to be involved in energy or electron transfer processes to SiNPs for an enhanced PL but usually provides some competing nonradiative relaxation channels at the interface of Si/SiO_2 to reduce the efficiency of excitation intended for PL centers.[60] So, the objects responsible for the variation in high energy excitation only lie on the chloroform and PF127. Using water as the reference, we measured the absorption spectra of pure chloroform and saturated PF127 aqueous solution (Figure 5). It can be clearly

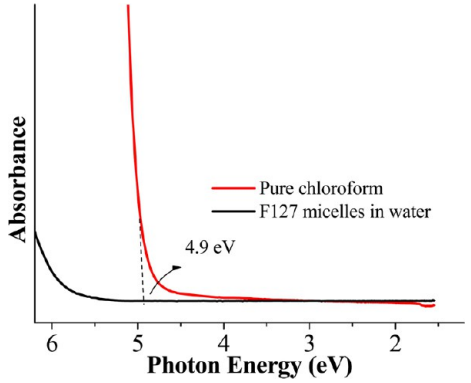

Figure 5. Absorption spectra of saturated PF127 aqueous solution and pure chloroform both recorded against water.

observed that PF127 is nearly transparent across the whole spectral region in 1−6 eV, while chloroform shows a steep rise of absorption at ∼4.9 eV, which matches the starting point of excitation quenching well. It can be, therefore, concluded that chloroform shields the soluble decyl-SiNPs from efficient excitation and/or efficiently relax the photogenerated charge carriers by adsorption to the surface of SiNPs. Over the literature reports,[18,19,23,24,62] chloroform or other common solvents were extensively used as dispersants of nanoscale silicon for optical measurements, including absorption and PL excitation spectra and were also found to have some effect on the PL. However, to the best of our knowledge, only a few reports paid attention to their high energy absorption as well as their correspondence to the spectral tail of silicon. The collected spectra actually reveal a whole effect of the solution including NPs and solvent to the passed incident light and did not reflect exactly the intrinsic optical properties of silicon by isolating interaction from the solvent. The resulting spectra are thereby deceptive and readily lend themselves to misinterpretation, particularly with regard to the origin of the PL and the real luminescence efficiency. Similar to ours, excitation spectra with one broad and strong band in near UV region, but with a dramatic decrease in deep UV region, have been reported; this is not the case for nanoscale silicon since the PL can be effectively initiated over the whole UV and VUV regions.[60,63,64]

In addition, during loading of decyl-SiNPs into the micelles, it was experimentally observed that the emission was significantly decreased when evaporating the chloroform solvent through a gentle nitrogen flow to yield the solid residue of decyl-SiNPs and PF127 copolymer. It is likely that at this stage the decyl-SiNPs were embedded into the disordered copolymer network, both PPO and PEO blocks interact with the decyl-SiNPs. However, the subsequent addition of HCl solution and stirring recovered the PL to a great extent. Over the latter process, it is believed that the polymeric surfactants start to self-assemble into a micellar structure and entrap the decyl-SiNPs into the hydrophobic PPO core regions. The above observations indicate that interaction of PEO block with decyl-SiNPs induced the PL quenching. The PL quenching of SiNPs by various solvents or chemicals is not so clear and still remains somewhat controversial.[8,65,66] By considering the transparency of PF127 ranging from the visible to ultraviolet region, herein it is speculated that interaction of PEO block with Si-based orbitals introduces states of appropriate energy for nonradiative quenching to occur while the PPO blocks did not play such a role of luminescent killer or at least did not significantly affect the SiNPs PL.

The stability and optical properties of the colloidal aqueous solution was further examined under various salt concentrations, pH values, and temperatures. As shown in Figure 6, NaCl concentration up to 1.0 M has no or little effect on the PL intensity and colloidal stability (Figure 6A). No flocculation

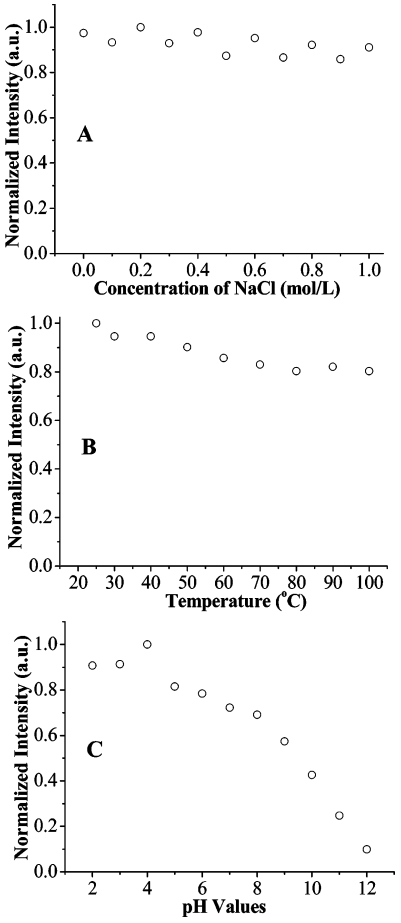

Figure 6. PL intensity from decyl-SiNPs@PF127@SiO_2 NP aqueous dispersion vs (A) concentration of NaCl, (B) temperature, and (C) pH under 270 nm excitation. In each panel, the intensity was normalized to its maximum. The emission spectra are shown in Supporting Information Figure S2.

of NPs was observed during the experiments. However, the PL intensity exhibits a clear dependence on the temperature and acidic-to-basic environment (Figure 6A and B). The PL intensity decreases slowly with increasing temperature, but the colloidal solution retains ~80% of its initial PL intensity even after being heated to 100 °C. In the acidic to basic pH environments, the PL intensity stays nearly constant under acidic conditions but is sensitive to basic solution. Indeed, an appreciable PL quenching was detected at pH 9 and total quenching occurred immediately at pH 12.

4. CONCLUSIONS

In summary, small sized SiNPs liberated from porous silicon and modified by decyl ligands through photoinduced hydrosilylation were encapsulated into silica cross-linked PF127 micelles via hydrophobic interaction. Due to the appropriate hydrodynamic size and organic surface capping of PEO blocks, these kinds of red-emitting silicon-based NPs may possess great potential in a variety of biomedical applications, particularly for in vivo studies. PL studies indicate that chloroform has a significant quenching effect for excitation above 4.9 eV by shielding the incident light or relaxing the charge carriers. This result highlights the importance of the interaction between solvents and silicon when studying excited processes, energy structures, and quantum confinement, etc., on the basis of optical spectra recorded from solution dispersions. The blocks of PEO in PF127 are also believed to participate in the PL quenching. The PL dependence studies on salt concentration (NaCl), temperature, and pH indicate that the colloidal aqueous solution is relatively stable to salt (NaCl) and temperature but sensitive to basic solution by appreciable PL quenching.

■ ASSOCIATED CONTENT

Ⓢ Supporting Information

PL emission spectra of the decyl-SiNPs@PF127@SiO_2 NP aqueous dispersion before and after 5 months of storage as well as the emission spectra versus concentration of NaCl, temperature, and pH. This material is available free of charge via the Internet at http://pubs.acs.org.

■ AUTHOR INFORMATION

Corresponding Author

*E-mail: guohui.pan@aliyun.com (G.-H.P.); rabah.boukherroub@iri.univ-lille1.fr (R.B.). Tel.: +33 3 62 53 17 24. Fax: +33 3 62 53 17 01.

Notes

The authors declare no competing financial interest.

■ ACKNOWLEDGMENTS

This work was financially supported by the Délégation Générale de l'Armement (DGA). G.P. thanks the Nord Pas-de-Calais region for a postdoctoral fellowship. The authors would like to thank Mariam Maaref (Hamamatsu Photonics, France) and Qi Wang for of PL quantum yields and UV–vis measurements. They also greatly acknowledge Ahmed Addad (Unité Matériaux et Transformations, UMR CNRS 8207, Université Lille 1, France) and Xiao-Dan Yu (Northeast Normal University, China) for the TEM measurements.

■ REFERENCES

(1) Canham, L. T. *Appl. Phys. Lett.* **1990**, *57*, 1046–1048.
(2) Sailor, M. J.; Lee, E. J. *Adv. Mater.* **1997**, *9*, 783–793.
(3) Cullis, A. G.; Canham, L. T.; Calcott, P. D. J. *J. Appl. Phys.* **1997**, *82*, 909–965.
(4) Lockwood, D. J. *Light Emission in Silicon from Physics to Devices*; Academic Press: New York, 1998.
(5) Veinot, J. G. C. *Chem. Commun.* **2006**, 4160–4168.
(6) Kang, Z.; Liu, Y.; Lee, S.-T. *Nanoscale* **2011**, *3*, 777–791.
(7) Li, Z. F.; Swihart, M. T.; Ruckenstein, E. *Langmuir* **2004**, *20*, 1963–1971.
(8) Kirkey, W. D.; Sahoo, Y.; Li, X.; He, Y.; Swihart, M. T.; Cartwright, A. N.; Bruckensteinc, S.; Prasad, P. N. *J. Mater. Chem.* **2005**, *15*, 2028–2034.
(9) Popplewell, J. F.; King, S. J.; Day, J. P.; Ackrill, P.; Fifield, L. K.; Cresswell, R. G.; Tada, M. L.; Liu, K. *J. Inorg. Biochem.* **1998**, *69*, 177–180.
(10) Bayllis, S. C.; Heald, R.; Fletcher, D. I.; Buckberry, L. D. *Adv. Mater.* **1999**, *11*, 318–321.
(11) Park, J. H.; Guo, L.; Maltzahn, G.; Ruoslahti, E.; Bhatia, S. N.; Sailor, M. J. *Nat. Mater.* **2009**, *8*, 331–336.
(12) Li, Z. F.; Ruckenstein, E. *Nano Lett.* **2004**, *4*, 1463–1467.
(13) Li, X.; He, Y.; Swihart, M. T. *Langmuir* **2004**, *20*, 4720–4727.
(14) Sato, S.; Swihart, M. T. *Chem. Mater.* **2006**, *18*, 4083–4088.
(15) Clark, R. J.; Dang, M. K. M.; Veinot, J. G. C. *Langmuir* **2010**, *26*, 15657–15664.
(16) Prtljaga, N.; D'Amato, E.; Pitanti, A.; Guider, R.; Froner, E.; Larcheri, S.; Scarpa, M.; Pavesi, L. *Nanotechnology* **2011**, *22*, 215704.
(17) Hua, F.; Swihart, M. T.; Ruckenstein, E. *Langmuir* **2005**, *21*, 6054–6062.
(18) Gupta, A.; Swihart, M. T.; Wiggers, H. *Adv. Funct. Mater.* **2009**, *19*, 696–703.
(19) Fan, J.; Chu, P. K. *Small* **2010**, *6*, 2080–2098.
(20) Erogbogbo, F.; Yong, K. T.; Roy, I.; Xu, G. X.; Prasad, P. N.; Swihart, M. T. *ACS Nano* **2008**, *2*, 873–878.
(21) Goller, B.; Polisski, S.; Wiggers, H.; Kovalev, D. *Appl. Phys. Lett.* **2010**, *96*, 211901.
(22) Henderson, E. J.; Shuhendler, A. J.; Prasad, P.; Baumann, V.; Maier-Flaig, F.; Faulkner, D. O.; Lemmer, U.; Wu, X. Y.; Ozin, G. A. *Small* **2011**, *7*, 2507–2516.
(23) Zhang, X.; Neiner, D.; Wang, S.; Louie, A. Y.; Kauzlarich, S. M. *Nanotechnology* **2007**, *18*, 095601.
(24) Hessel, C. M.; Rasch, M. R.; Hueso, J. L.; Goodfellow, B. W.; Akhavan, V. A.; Puvanakrishnan, P.; Tunnel, J. W.; Korgel, B. A. *Small* **2010**, *6*, 2026–2034.
(25) Harum, N. A.; Horrocks, B. R.; Fulton, D. A. *Nanoscale* **2011**, *3*, 4733–4741.
(26) Popović, Z.; Liu, W.; Chauhan, V. P.; Lee, J.; Wong, C.; Greytak, A. B.; Insin, N.; Nocera, D. G.; Fukumura, D.; Jain, R. K.; Bawendi, M. G. *Angew. Chem., Int. Ed.* **2010**, *49*, 8649–8652.
(27) Huo, Q.; Liu, J.; Wang, L.-Q.; Jiang, Y.; Lambert, T. N.; Fang, E. *J. Am. Chem. Soc.* **2006**, *128*, 6447–6453.
(28) Zanarini, S.; Rampazzo, E.; Bonacchi, S.; Juris, R.; Marcaccio, M.; Montalti, M.; Paolucci, F.; Prodi, L. *J. Am. Chem. Soc.* **2009**, *131*, 14208–14209.
(29) Rampazzo, E.; Bonacchi, S.; Juris, R.; Montalti, M.; Genovese, D.; Zaccheroni, N.; Prodi, L.; Rambaldi, D. C.; Zattoni, A.; Reschiglian, P. *J. Phys. Chem. B* **2010**, *114*, 14605–14613.
(30) Genovese, D.; Montalti, M.; Prodi, L.; Rampazzo, E.; Zaccheroni, N.; Tosic, O.; Altenhöner, K.; Mayb, F.; Mattay, J. *Chem. Commun.* **2011**, *47*, 10975–10977.
(31) Valenti, G.; Rampazzo, E.; Bonacchi, S.; Khajvand, T.; Juris, R.; Montalti, M.; Marcaccio, M.; Paolucci, F.; Prodi, L. *Chem. Commun.* **2012**, *48*, 4187–4189.
(32) Liu, Z.; Ding, J.; Xue, J. *New J. Chem.* **2009**, *33*, 88–92.
(33) Shishido, S. M.; Seabra, A. B.; Loh, W.; de Oliveira, M. G. *Biomaterials* **2003**, *24*, 3543–3553.
(34) Wilcoxon, J. P.; Samara, G. A.; Provencio, P. N. *Phys. Rev. B* **1999**, *60*, 2704–2714.
(35) Warner, J. H.; Hoshino, A.; Yamamoto, K.; Tilley, R. D. *Angew. Chem., Int. Ed.* **2005**, *44*, 4550–4554.

(36) Rosso-Vasic, M.; Spruijt, E.; van Lagen, B.; Cola, L. D.; Zuilhof, H. *Small* **2008**, *4*, 1835−1841.
(37) Gupta, A.; Wiggers, H. *Nanotechnology* **2011**, *22*, 055707.
(38) Godefroo, S.; Hayne, M.; Jivanescu, M.; Stesmans, A.; Zacharias, M.; Lebedev, O. I.; van Tendelooand, G.; Moshchalkov, V. V. *Nat. Nanotechnol.* **2008**, *3*, 174−178.
(39) Dasog, M.; Yang, Z.; Regli, S.; Atkins, T. M.; Faramus, A.; Singh, M. P.; Muthuswamy, E.; Kauzlarich, S. M.; Tilley, R. D.; Veinot, J. G. C. *ACS Nano* **2013**, *7*, 2676−2685.
(40) Wang, R.; Pi, X.; Yang, D. *J. Phys. Chem. C* **2012**, *116*, 19434−19443.
(41) Dohnalová, K.; Fučíková, A.; Umesh, C. P.; Humpolíčková, J.; Paulusse, J. M. J.; Valenta, J.; Zuilhof, H.; Hof, M.; Gregorkiewicz, T. *Small* **2012**, *8*, 3185−3191.
(42) Dohnalová, K.; Poddubny, A. N.; Prokofiev, A. A.; de Boer, A. M. W. D.; Umesh, C. P.; Paulusse, J. M. J.; Zuilhof, H.; Gregorkiewicz, T. *Light Sci. Appl.* **2013**, *2*, e47.
(43) Gaponik, N.; Hickey, S. G.; Dorfs, D.; Rogach, A. L.; Eychmüller, A. *Small* **2010**, *6*, 1364−1378.
(44) Kolasinski, K. W.; Hartline, J. D.; Kelly, B. T.; Yadlovskiy, J. *Mol. Phys.* **2010**, *108*, 1033−1043.
(45) Boukherroub, R.; Wojtyk, J. T. C.; Wayner, D. D. M.; Lockwood, D. J. *J. Electrochem. Soc.* **2002**, *149*, H59−H63.
(46) Nahidi, M.; Kolasinski, K. W. *J. Electrochem. Soc.* **2006**, *153*, C19−C26.
(47) Dudley, M. E.; Kolasinski, K. W. *Phys. Status Solidi A* **2009**, *206*, 1240−1244.
(48) Dudley, M. E.; Kolasinski, K. W. *Electrochem. Solid-State Lett.* **2009**, *12*, D22−D26.
(49) Yang, C.-S.; Bley, R. A.; Kauzlarich, S. M.; Lee, H. W. H.; Delgado, G. R. *J. Am. Chem. Soc.* **1999**, *121*, 5191−5195.
(50) Cui, S.; Chen, H.; Zhu, H.; Tian, J.; Chi, X.; Qian, Z.; Achilefu, S.; Gu, Y. *J. Mater. Chem.* **2012**, *22*, 4861−4873.
(51) Wu, Z.; Guo, C.; Liang, S.; Zhang, H.; Wang, L.; Sun, H.; Yang, B. *J. Mater. Chem.* **2012**, *22*, 18596−18602.
(52) Jurbergs, D.; Rogojina, E.; Mangolini, L.; Kortshagen, U. *Appl. Phys. Lett.* **2006**, *88*, 233116.
(53) Qu, L. H.; Peng, X. G. *J. Am. Chem. Soc.* **2002**, *124*, 2049−2055.
(54) Peng, X.; Schlamp, M. C.; Kadavanich, A. V.; Alivisatos, A. P. *J. Am. Chem. Soc.* **1997**, *119*, 7019−7029.
(55) Lam, Y. M.; Grigorieff, N.; Goldbeck-Wood, G. *Phys. Chem. Chem. Phys.* **1999**, *1*, 3331−3334.
(56) Delerue, C.; Allan, G.; Lannoo, M. *Phys. Rev. B* **1993**, *48*, 11024−11036.
(57) Delerue, C.; Allan, G.; Lannoo, M. *J. Lumin.* **1999**, *80*, 65−73.
(58) Reboredo, F. A.; Franceschetti, A.; Zunger, A. *Appl. Phys. Lett.* **1999**, *75*, 2972−2974.
(59) Ledoux, G.; Guillois, O.; Porterat, D.; Reynaud, C.; Huisken, F.; Kohn, B.; Paillard, V. *Phys. Rev. B* **2000**, *62*, 15942−15951.
(60) Pankratov, V.; Osinniy, V.; Kotlov, A.; Larsen, A. N.; Nielsen, B. B. *Phys. Rev. B* **2011**, *83*, 045308.
(61) Wilcoxon, J. P.; Samara, G. A.; Provencio, P. N. *Phys. Rev. B* **1999**, *60*, 2704−2714.
(62) Mastronardi, M. L.; Hennrich, F.; Henderson, E. J.; Maier-Flaig, F.; Blum, C.; Reichenbach, J.; Lemmer, U.; Kübel, C.; Wang, D.; Kappes, M. M.; Ozin, G. A. *J. Am. Chem. Soc.* **2011**, *133*, 11928−11931.
(63) Chao, Y.; Krishnamurthy, S.; Montalti, M.; Lie, L. H.; Houlton, A.; Horrocks, B. R.; Kjeldgaard, L.; Dhanak, V. R.; Hunt, M. R. C.; Šiller, L. *J. Appl. Phys.* **2005**, *98*, 044316.
(64) Chao, Y.; Houlton, A.; Horrocks, B. R.; Hunt, M. R. C.; Poolton, N. R. J.; Yang, J.; Šiller, L. *Appl. Phys. Lett.* **2006**, *88*, 263119.
(65) Chun, J. K. M.; Bocarsly, A. B.; Cottrell, T. R.; Benziger, J. B.; Yees, J. C. *J. Am. Chem. Soc.* **1993**, *115*, 3024−3025.
(66) Rehm, J. M.; Lendon, G. L. M.; Fauchet, P. M. *J. Am. Chem. Soc.* **1996**, *118*, 4490−4491.